THE JOURNAL OF BIOLOGICAL CHEMISTRY
Vol. 279, No. 11, Issue of March 12, pp. 10215–10221, 2004

Printed in U.S.A.

Locking the β_3 Integrin I-like Domain into High and Low Affinity Conformations with Disulfides*

Received for publication, November 20, 2003
Published, JBC Papers in Press, December 16, 2003, DOI 10.1074/jbc.M312732200

Bing-Hao Luo, Junichi Takagi‡, and Timothy A. Springer§

From the CBR Institute for Biomedical Research and Department of Pathology, Harvard Medical School, Boston, Massachusetts 02115

Although integrin α subunit I domains exist in multiple conformations, it is controversial whether integrin β subunit I-like domains undergo structurally analogous movements of the α7-helix that are linked to affinity for ligand. Disulfide bonds were introduced into the β_3 integrin I-like domain to lock its β6-α7 loop and α7-helix in two distinct conformations. Soluble ligand binding, ligand mimetic mAb binding and cell adhesion studies showed that disulfide-bonded receptor $\alpha_{IIb}\beta_3^{T329C/A347C}$ was locked in a low affinity state, and dithiothreitol treatment restored the capability of being activated to high affinity binding; by contrast, disulfide-bonded $\alpha_{IIb}\beta_3^{V332C/M335C}$ was locked in a high affinity state. The results suggest that activation of the β subunit I-like domain is analogous to that of the α subunit I domain, *i.e.* that axial movement in the C-terminal direction of the α7-helix is linked to rearrangement of the I-like domain metal ion-dependent adhesion site into a high affinity conformation.

Integrins are large heterodimeric adhesion molecules that convey signals bidirectionally across the plasma membrane (1, 2). Both integrin subunits are type I transmembrane proteins with large extracellular domains. Priming of the extracellular domain for ligand binding (*i.e.* increasing its affinity for ligand) is initiated by moving apart the α and β subunit cytoplasmic domains and probably separation of the transmembrane domains as well (3). Conversely, binding of ligand can also initiate cytoplasmic domain separation (3); the equilibria relating conformational change and ligand binding are linked (4). The low affinity integrin conformation is highly bent, with the headpiece that contains the ligand binding domains in an extensive interface with the tailpiece that contains the α and β subunit legs (4–8) (Fig. 1*A*). After priming or ligand binding, a switchblade-like opening extends the headpiece away from the membrane (4, 7) (Fig. 1, *B* and *C*). In extended integrins, two conformations of the headpiece are seen. The open conformation of the headpiece (Fig. 1*C*) is present when ligand is bound and differs from the closed conformation (Fig. 1*B*) in the presence of an obtuse angle between the β-subunit hybrid and I-like domains (4, 8). Recently, we mutationally introduced *N*-glycosylation sites into the interface of the hybrid and I-like domains to stabilize the open headpiece. The wedged-open mutants exhibited constitutively high affinity for ligand and adopted an extended conformation (9).

We have proposed that the change in affinity at the ligand binding site in the I-like domain around its metal ion-dependent adhesion site (MIDAS)[1] is communicated to the interface with the hybrid domain on the opposite end of the I-like domain by axial displacement in the C-terminal direction of the I-like domain α7-helix (4, 8, 9) (Fig. 1, *B* and *C*). The β-subunit I-like domain is inserted in the hybrid domain, and thus these domains have two interconnections. A piston-like movement at the I-like α7-helix connection and pivoting about the other connection would yield a swing at the I-like-hybrid domain interface approximating that seen in electron microscopy studies (4, 8). One basis for proposing this mechanism for communicating a change in affinity to the I-like domain MIDAS is that the structurally homologous I domain inserted in some integrin α subunits undergoes a similar piston-like movement of its C-terminal α7-helix, which regulates the affinity of its MIDAS for ligand (2).

There is controversy concerning this proposed mechanism. Soaking of a ligand-mimetic Arg-Gly-Asp (RGD) peptide into integrin $\alpha_V\beta_3$ crystals, in which $\alpha_V\beta_3$ was constrained in the bent conformation by lattice contacts, induced β6-α7 loop and α1-helix movements, but not α7-helix displacement (5). It was therefore suggested that α I and β I-like domains are activated by distinct mechanisms. Demonstration of movement of an epitope in the α1-helix was used to support the hypothesis that the mechanism of I-like domain activation differs from that of the I domain (10). On the other hand, conformational change at this region would not contradict C-terminal α7-helix movement, and the mutation L358A in the α7-helix of the β_1 I-like domain causes activation, supporting some type of conformational change around the α7-helix upon ligand binding (11). Furthermore, solution x-ray scattering studies and exposure of epitopes on the inner side of the hybrid domain in the presence of ligand (11, 12) support the direct observations of hybrid domain swing-out (4, 8).

Here, we directly test the hypothesis that specific rearrangements occur in the β6-α7 loop and α7-helix of β I-like domains that are structurally analogous to those that occur in α I domains and are linked to integrin activation. Disulfide bonds have previously been introduced into α I domains to constrain

* This work was supported by National Institutes of Health Grant HL48675 (to T. A. S. and J. T). The costs of publication of this article were defrayed in part by the payment of page charges. This article must therefore be hereby marked "*advertisement*" in accordance with 18 U.S.C. Section 1734 solely to indicate this fact.

‡ Present address: Institute for Protein Research, Laboratory of Protein Synthesis and Expression, Osaka University, 3-2 Yamadaoka, Suita, Osaka 565-0871, Japan.

§ To whom correspondence may be addressed: CBR Institute for Biomedical Research and Department of Pathology, Harvard Medical School, 200 Longwood Ave., Boston, MA 02115. Tel.: 617-278-3200; Fax: 617-278-3232; E-mail: springeroffice@cbr.med.harvard.edu.

[1] The abbreviations used are: MIDAS, metal ion-dependent adhesion site; TBS, Tris-buffered saline; DTT, dithiothreitol; biotin-BMCC, 1-biotinamido-4 (4′-[maleimodoethyl-cyclohexane]-carboxamido)butane; FITC, fluorescein isothiocyanate; HBS, Hepes-buffered saline; BSA, bovine serum albumin; mAb, monoclonal antibody; CHO, Chinese hamster ovary.

the β6-α7 loop and α7-helix. The α_L (13–16) and α_M (17) I domains have been locked into closed, intermediate, or open conformers with low, intermediate, or high affinity for ligand, respectively. Crystal structure studies on the mutant α_L I domains confirmed alterations in the β6-α7 loop corresponding to α7-helix displacements of one and two turns of helix in the intermediate and open conformations, respectively (16). The disulfide-constrained, high affinity, open conformation of the α_L I domain corresponds precisely in the critical β6-α7 loop and MIDAS loops to the open conformation of the wild-type α_2 and α_M I domains seen when this conformation was stabilized in crystals by ligand or ligand-like lattice contacts (18, 19). The studies reported here on the β I-like domain show that disulfide bonds mutationally introduced into the β6/α7 region lock integrins that lack I domains into two distinct affinity states. The data uniquely support the proposal that downward movement of the α7-helix induces I-like domain activation and demonstrate that α I and β I-like domains are activated by structurally analogous mechanisms.

MATERIALS AND METHODS

High Affinity I-like Domain Model—The model was built with the Segmod module (20) of GeneMine version 3.5 using residues 108–333 and 347–353 of Protein Data Bank accession number 1JV2 (6) as template and aligning them with residues 108–333 and 340–346 of the model sequence, respectively. This corresponded to a 7-residue, 2-turn displacement of the α7-helix along its helical axis; residues 334–339 were left nontemplated.

Plasmid Construction, Transient Transfection, and Immunoprecipitation—Plasmids coding for full-length human α_{IIb} and β_3 were subcloned into pEF/V5-HisA or pcDNA3.1/Myc-His(+) as described previously (4). Mutants were made using site-directed mutagenesis with the QuikChange kit (Stratagene, La Jolla, CA), and DNA sequences were confirmed before being transfected into 293T cells using calcium phosphate precipitates (21). Transfected cells were metabolically labeled with [^{35}S]cysteine/methionine as described (4). Lysates in 20 mM Tris-buffered saline, pH 7.4 (TBS), supplemented with 1 mM Ca^{2+}, 1 mM Mg^{2+}, 1% Triton X-100, and 0.1% Nonidet P-40 were immunoprecipitated with 1 μg of anti-β_3 mAb AP3 and protein G-Sepharose at 4 °C for 1 h and subjected to nonreducing SDS 7.5% PAGE and fluorography (22).

Labeling of Free Cysteines and Western Blotting—Transiently transfected 293T cells, treated with or without 5 mM DTT at 37 °C for 30 min in TBS containing 1 mM Ca^{2+}, followed by washing with TBS plus 1 mM Ca^{2+} three times, were labeled with 400 μM 1-biotinamido-4 (4′-[maleimidoethyl-cyclohexane]-carboxamido)butane (biotin-BMCC) (Pierce) at room temperature for 30 min, washed with TBS plus 1 mM Ca^{2+} three times, and lysed with TBS with 1% Triton X-100 and 0.1% Nonidet P-40. $\alpha_{IIb}\beta_3$ was immunoprecipitated with AP3 mAb-Sepharose at 4 °C for 1 h and subjected to SDS 7.5% PAGE. Samples were transferred to polyvinylidene difluoride membranes and probed with 2 μg/ml horseradish peroxidase-conjugated avidin at 20 °C for 30 min or with 2 μg/ml anti-*myc* antibody (Invitrogen) for 30 min at 20 °C, followed by washing and 2 μg/ml horseradish peroxidase-conjugated anti-mouse-IgG (Zymed Laboratories Inc., San Francisco, CA) for 30 min at 20 °C, and then detected by chemiluminescence using the ECL Western blotting kit (Amersham Biosciences). BioMax film (Eastman Kodak Co.) was exposed for about 20 s. The film was scanned using DUOSCAN 1200 (Agfa, Mortsel, Belgium), and data were saved as a tiff file. NIH Image 1.62 (NIMH, National Institutes of Health, Bethesda, MD) was used to determine the intensity of each band within identical rectangular areas. After subtracting the intensity of mock transfectants in the same areas, the ratio of the intensity of BMCC and *myc* bands was determined.

Two-color Ligand Binding Assay on 293T Transfectants—Binding of FITC-labeled human fibrinogen was determined as described (4). Briefly, transiently transfected 293T cells in 20 mM Hepes-buffered saline (pH 7.4) (HBS) supplemented with 5.5 mM glucose and 1% BSA were incubated with 60 μg/ml fluorescein-labeled fibrinogen in the presence of 1 mM EDTA, 5 mM Ca^{2+}, or 1 mM Ca^{2+} plus 10 μg/ml PT25-2 mAb at 20 °C for 30 min, and then 10 μg/ml Cy3-labeled mAb AP3 was added, and cells were incubated on ice for another 30 min before being subjected to flow cytometry. Fibrinogen binding was expressed as a percentage of the mean fluorescence intensity of FITC-fibrinogen relative to that of staining with AP3 mAb.

Expression and Ligand Binding Activity of $\alpha_{IIb}\beta_3$ on CHO-K1 Transfectants—The plasmids described above coding for α_{IIb} and β_3 were introduced into CHO-K1 cells using calcium phosphate precipitates (21). Transfectants were selected with 5 mg/ml G418. After 2 weeks, the cells were stained with AP3 mAb and subjected to fluorescence-activated cell sorting to obtain lines expressing the desired level of $\alpha_{IIb}\beta_3$. Prior to ligand binding, transfected cells were suspended in HBS supplemented with 5.5 mM glucose and 1% BSA and incubated with 1 mM EDTA, 5 mM Ca^{2+}, or 1 mM Ca^{2+} plus 10 μg/ml PT25-2, with or without 5 mM DTT, at 20 °C for 30 min. Staining with fluorescein-labeled human fibrinogen and the ligand mimetic PAC-1 mAb (Becton Dickinson, San Jose, CA) was measured as described (4).

Cell Adhesion to Immobilized Fibrinogen—Cell adhesion was assayed as described (23). Briefly, transfected CHO-K1 cells were labeled with 2′,7′-bis-(carboxyethyl)-5(and-6)-carboxyfluorescein (Molecular Probes, Inc., Eugene, OR) and suspended to 10^6/ml in HBS supplemented with 5.5 mM glucose, 1% BSA, and either 1 mM EDTA, 5 mM Ca^{2+}, or 5 mM DTT plus 5 mM Ca^{2+}. Cell suspensions were incubated in wells that had been coated with different concentrations of fibrinogen followed by blocking with 1% BSA. After incubation at 37 °C for 1 h, unbound cells were washed off after three resuspensions with a multichannel pipette. The fluorescence of input cells and bound cells in each well was quantitated on a fluorescent concentration analyzer (Idexx, Westbrook, ME). Bound cells were expressed as a percentage of total input cells.

LIBS Expression—Anti-LIBS mAbs LIBS-1, LIBS-6, and PMI-1 were kind gifts of M. H. Ginsberg (Scripps Research Institute, La Jolla, CA). LIBS expression was measured as described (9). In brief, CHO-K1 cells stably expressing wild type or mutant $\alpha_{IIb}\beta_3$ in HBS supplemented with 5.5 mM glucose and 1% BSA were incubated under different conditions as indicated in the legend to Fig. 5 for 30 min at 20 °C. LIBS mAbs were added to a final concentration of 10 μg/ml, and cells were incubated on ice for another 30 min before staining with FITC-conjugated anti-mouse IgG and flow cytometry.

RESULTS

Design of I-like Domains Locked in Low Affinity and High Affinity Conformations—We hypothesized that in both the unliganded and liganded $\alpha_V\beta_3$ structures (5, 6), the C-terminal α7-helix of the β_3 I-like domain is in a position stabilizing a closed, low affinity conformation; therefore, these structures were used to design low affinity mutants. An open, high affinity conformation was modeled assuming that the α7-helix was displaced in the C-terminal axial direction by two α-helical turns (see "Materials and Methods"). The distance between Cβ atoms of Thr^{329} and Ala^{347} in the unliganded and RGD-liganded $\alpha_V\beta_3$ structures is 4.4 and 4.9 Å, respectively, whereas it is 9.6 Å in the hypothesized high affinity model. Therefore, the mutant $\beta_3^{T329C/A347C}$ was expected to form a disulfide bond in the low but not the high affinity conformation and to be stabilized in the low affinity, closed conformation (Fig. 1, *D* and *F*). On the other hand, the distance between the Cβ atoms of Val^{332} and Met^{335} in the unliganded and RGD-liganded $\alpha_V\beta_3$ structures is 10.0 and 8.3 Å, respectively, whereas it is 3.7 Å in the hypothesized high affinity model. Therefore, the mutant $\beta_3^{V332C/M335C}$ was expected to form a disulfide bond in the high but not the low affinity conformation (Fig. 1, *E* and *G*) and to be stabilized in the high affinity, open conformation.

Expression of Wild Type and Mutant $\alpha_{IIb}\beta_3$ Receptors and Formation of Disulfide Bonds—Wild type and mutant β_3 subunits were co-transfected with wild type α_{IIb} in 293T cells and subjected to immunostaining flow cytometry (Fig. 2, *A* and *B*). The wild type and mutant receptors were recognized equally well by mAb to epitopes constitutively present on the α_{IIb} and β_3 subunits, including AP3 (anti-β_3), 10E5 (anti-α_{IIb}), HA5 (anti-α_{IIb}), and AP2 (anti-$\alpha_{IIb}\beta_3$ complex-specific) (Fig. 2*A*), suggesting that the two mutant receptors adopted a native fold on the cell surface. However, the mutant $\beta_3^{V332C/M335C}$ receptor was recognized weakly by anti-β_3 mAb 7E3 (Fig. 2*B*). The 7E3 mAb recognizes residues in the specificity-determining, β2-β3 loop near the β_3 I-like MIDAS (24). Since the single cysteine mutants β_3^{V332C} and β_3^{M335C} were recognized by 7E3 (Fig. 2*B*),

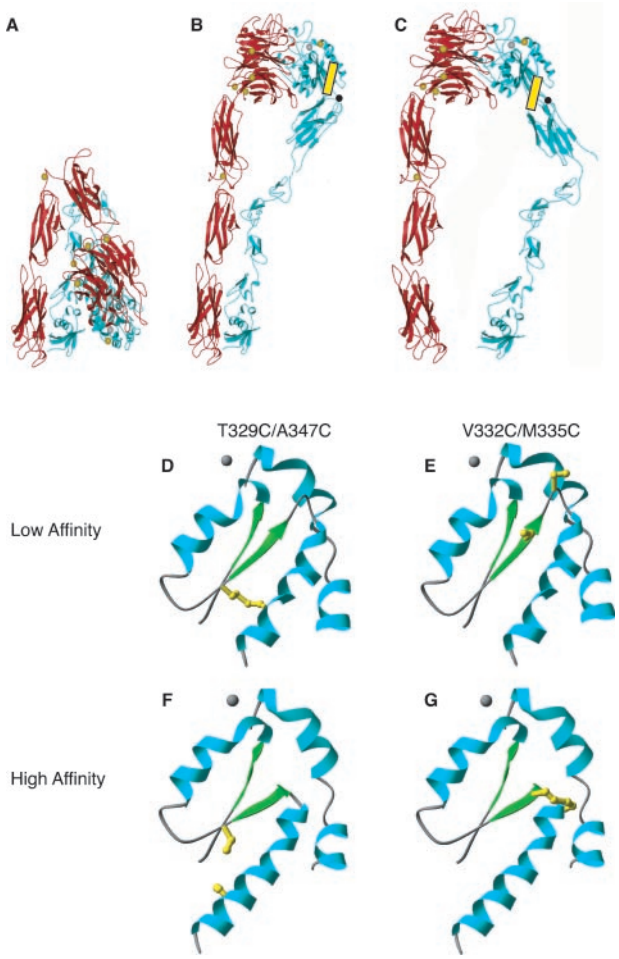

FIG. 1. **Model of integrin activation and design of mutant β_3 I-like domains.** *A–C*, model for integrin activation, with at least three conformations of the extracellular domain (4). *A*, bent, low affinity conformation. *B*, extended conformation with closed headpiece. *C*, extended conformation with open headpiece. The outward swing of the hybrid domain is hypothesized to result from downward movement of the I-like domain α7-helix (*yellow cylinder*) and pivoting about the other β I-like-hybrid domain connection at about residue 106 (*black circle*). *D–G*, design of mutants of the β_3 I-like domain. For clarity, only two segments of the I-like domain, from the β1-α1 loop to the α1-helix and from the β5-strand to the α7-helix are shown. Cysteine substitutions (*yellow stick* and *ball*) were modeled with SwissPdb Viewer (28). The MIDAS metal ion (*silver sphere*) (5) is added to identify the ligand binding site. *D*, low affinity structure with T329C/A347C mutation. *E*, low affinity structure with V332C/M335 mutation. *F*, high affinity model with T329C/A347C mutation. *G*, high affinity model with V332C/M335C mutation. The low affinity structure is from IJV2; the high affinity model is described under "Materials and Methods." This *figure* was prepared with RIBBONS (29).

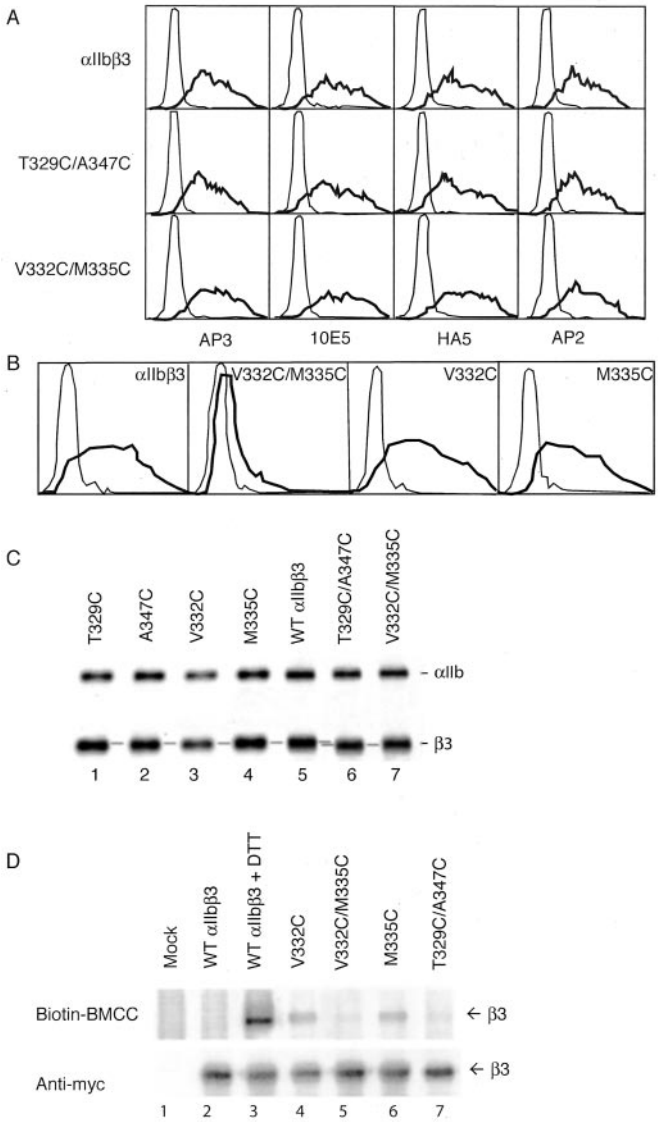

FIG. 2. **Expression of mutant $\alpha_{IIb}\beta_3$ integrins on 293T cells and formation of disulfide bonds.** *A* and *B*, immunofluorescent flow cytometry. *A*, 293T transfectants were labeled with AP3 (anti-β_3), 10E5 (anti-α_{IIb}), HA5 (anti-α_{IIb}), and AP2 (anti-$\alpha_{IIb}\beta_3$ complex-specific). *Thick* and *thin lines* show labeling of the $\alpha_{IIb}\beta_3$ transfectant and the mock transfectant, respectively. *B*, labeling with 7E3 mAb (*thick line*) or X63 control IgG1 (*thin line*). *C*, immunoprecipitation. Lysates from ^{35}S-labeled 293T cell transfectants were immunoprecipitated with mAb AP3. Precipitates were subjected to nonreducing SDS-7.5% PAGE and fluorography. *Segments* of *straight lines* drawn through the β_3 bands in *lanes 1–5* and *lanes 6* and *7* are shown *between lanes* to emphasize the difference in migration. *D*, labeling of free cysteines. Transfected cells were treated with (wild-type only) or without 5 mM DTT at 37 °C for 30 min and labeled with biotin-BMCC at room temperature for 30 min. Immunoprecipitates with AP3 mAb-Sepharose were subjected to nonreducing 7.5% SDS-PAGE. Western blotting was with HRP-avidin to detect biotin-BMCC or anti-*myc* mAb to detect the *myc*-tagged β_3 subunit.

the conformational change induced by the disulfide bond formed between V332C and M335C (see below) appears to diminish the 7E3 epitope. By contrast, mutant $\beta_3^{T329C/A347C}$ was well recognized by 7E3 (data not shown) (see Fig. 4*A*).

Nonreducing SDS-PAGE of ^{35}S-labeled, immunoprecipitated receptors showed that the α_{IIb} subunits migrated similarly (Fig. 2*C*), whereas the mutant $\beta_3^{T329C/A347C}$ and $\beta_3^{V332C/M335C}$ subunits (Fig. 2*C*, *lanes 6* and *7*) migrated slightly faster than wild type β_3 (Fig. 2*C*, *lane 5*). By contrast, all β_3 single cysteine mutants migrated similarly to wild-type β_3 (Fig. 2*C*, *lanes 1–4*). In general, disulfide bonds increase the mobility of proteins in SDS-PAGE, and these results suggest that the cysteines introduced into the $\beta_3^{T329C/A347C}$ and $\beta_3^{V332C/M335C}$ mutants form a disulfide bond.

To confirm disulfide bond formation, free sulfhydryls were labeled with the maleimide-containing reagent, biotin-BMCC. The idea was that introducing a single cysteine should increase labeling, whereas introducing two cysteines would not increase labeling if they formed a disulfide bond. Transfectants were treated with biotin-BMCC, lysed, immunoprecipitated with AP3 mAb to $\alpha_{IIb}\beta_3$, and subjected to SDS-PAGE and blotting with avidin (Fig. 2*D*). The β_3 subunit was fused at its C terminus to a *myc* tag, and blotting with a *myc* mAb was used as a control for β_3 loading. Whereas wild-type $\alpha_{IIb}\beta_3$ showed almost no biotin labeling (Fig. 2*D*, *lane 2*), the $\alpha_{IIb}\beta_3$ single cysteine mutants V332C and M335C showed marked labeling (Fig. 2*D*,

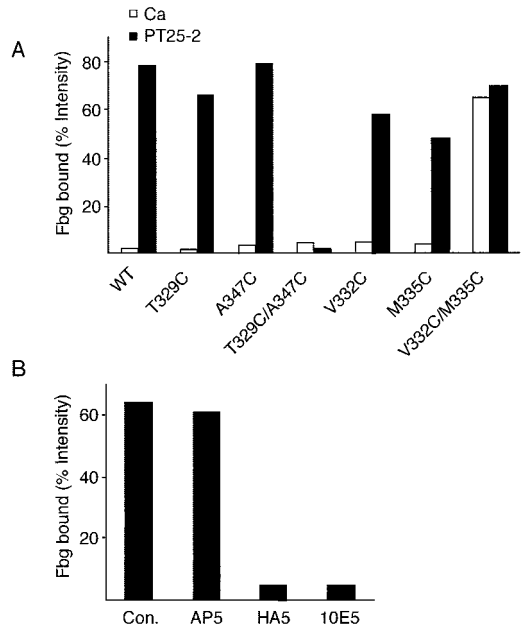

FIG. 3. **Ligand binding activity of mutant $\alpha_{IIb}\beta_3$ integrins on 293T cells.** *A*, soluble fibrinogen binding of 293T cell transfectants in the presence of 5 mM Ca^{2+} (*white bar*) or 1 mM Ca^{2+} plus 10 μg/ml PT25-2 (*black bar*) at room temperature for 30 min. *B*, effect of mAbs. Soluble fibrinogen binding in the presence of 5 mM Ca^{2+} was measured in presence of activating LIBS antibody AP5 or blocking antibodies HA5 and 10E5. The control is with X63 IgG1. Fibrinogen binding was measured with two-color immunofluorescence as described under "Materials and Methods" and is expressed as the mean fluorescence intensity of fibrinogen staining as a percentage of mean fluorescence intensity of staining with AP3 mAb.

lanes 4 and *6*). The cysteines introduced in the V332C/M335C and T329C/A347C mutants clearly formed disulfides, because labeling was at the same level as the wild type (Fig. 2*D*, *lanes 5* and *7*), whereas it would have been twice that of the single cysteine mutants if disulfides had not formed. To estimate the number of free cysteines per β_3 subunit, the ratio of the intensity of avidin binding to that of anti-*myc* binding was determined. As an additional control, wild-type $\alpha_{IIb}\beta_3$ on the transfectants was treated with 5 mM DTT for 30 min at 37 °C. The avidin/anti-*myc* ratios for the wild type, wild type with DTT treatment, β_3^{V332C}, $\beta_3^{V332C/M335C}$, β_3^{M335C}, and $\beta_3^{T329C/A347C}$ subunits were 0.05, 0.82, 0.20, 0.04, 0.19, and 0.04, respectively. If β_3^{V332C} is assumed to have one additional free cysteine sulfhydryl compared with wild type, then β_3^{M335C} also has 1.0 additional free cysteine, $\beta_3^{V332C/M335C}$ and $\beta_3^{T329C/A347}$ have no additional free β_3 cysteines, and wild type $\alpha_{IIb}\beta_3$ treated with DTT has 5.2 free cysteines. By contrast, there are a total of 54 cysteines in wild type β_3.

Ligand Binding Properties of 293T Transfectants with Disulfide-locked Receptors—Binding to soluble fibrinogen was first examined using two-color flow cytometry (4) in transiently transfected 293T cells, in which wild type $\alpha_{IIb}\beta_3$ basally has low affinity for ligand. Wild type $\alpha_{IIb}\beta_3$ bound fibrinogen when stimulated with the activating mAb PT25-2 but not basally in Ca^{2+} (Fig. 3*A*). Each of the four single cysteine mutants behaved similarly to the wild type receptor (Fig. 3*A*). By contrast, the putative locked closed, double cysteine mutant $\alpha_{IIb}\beta_3^{T329C/A347C}$ did not bind soluble fibrinogen even in the presence of PT25-2 (Fig. 3*A*). Furthermore, the putative locked open mutant $\alpha_{IIb}\beta_3^{V332C/M335C}$ bound soluble fibrinogen even in Ca^{2+}, and the addition of PT25-2 mAb did not further increase binding (Fig. 3*A*). Constitutive binding in Ca^{2+} by the $\alpha_{IIb}\beta_3^{V332C/M335C}$ mutant was abolished by two blocking α_{IIb} mAbs, HA5 and 10E5, but neither blocked nor further activated by the activating β_3 mAb AP5 (Fig. 3*B*), confirming that the high affinity binding of the transfected cells was specific.

Functional Properties of Mutant Receptors in CHO-K1 Transfectants—To further examine the disulfide-locked receptors, stable CHO-K1 transfectants were established, and clones were selected that expressed similar quantities of wild-type $\alpha_{IIb}\beta_3$, $\alpha_{IIb}\beta_3^{T329C/A347C}$, and $\alpha_{IIb}\beta_3^{V332C/M335C}$. The transfectants were recognized equally well by a panel of mAb to constitutively expressed α_{IIb}, β_3, and $\alpha_{IIb}\beta_3$ epitopes, with the exception of 7E3 mAb (Fig. 4*A*). Mutant $\alpha_{IIb}\beta_3^{V332C/M335C}$ blunted but did not completely abolish the binding of 7E3.

CHO-K1 transfectants expressing the wild type receptor did not bind soluble fibrinogen or PAC-1 in Ca^{2+} but bound when stimulated by activating mAb PT25-2 (Fig. 4, *B* and *C*). Treatment with 5 mM DTT at 20 °C for 30 min slightly increased ligand binding to wild type $\alpha_{IIb}\beta_3$ in Ca^{2+}, but this binding was much less than that seen with PT25-2 mAb with or without DTT treatment. Mutant $\alpha_{IIb}\beta_3^{T329C/A347C}$ did not bind fibrinogen or PAC-1 basally, and binding was not stimulatable with PT25-2. However, DTT treatment restored the ability of PT25-2 to stimulate fibrinogen and PAC-1 binding (Fig. 4, *B* and *C*), suggesting that the Cys^{329}–Cys^{347} disulfide bond locked the I-like domain in the closed conformation, and this constraint was released by DTT treatment. By contrast, mutant $\alpha_{IIb}\beta_3^{V332C/M335C}$ showed high binding to soluble fibrinogen and PAC-1, and binding was not further increased by activation. DTT treatment did not reduce fibrinogen or PAC-1 binding of the $\alpha_{IIb}\beta3^{V332C/M335C}$ mutant in Ca^{2+}, probably because the Cys^{332}–Cys^{335} disulfide bond was stable to reduction under nondenaturing conditions like the vast majority of the native disulfides in β_3.

The affinity state of disulfide-bonded mutants was further tested in cell adhesion assays on immobilized fibrinogen. High affinity is required for binding to soluble ligand or ligand mimetic mAbs. In contrast, wild type $\alpha_{IIb}\beta_3$ can mediate cell adhesion to immobilized fibrinogen in the absence of activation, as long as high coating concentrations above 1 μg/ml of fibrinogen are used (Fig. 4*D*), consistent with our previous report (9). DTT treatment slightly increased the avidity of the wild type receptor, as shown by a shift in the dose-response curve. In contrast, mutant $\alpha_{IIb}\beta_3^{T329C/A347C}$ did not adhere even at the highest coating concentration of fibrinogen, whereas DTT treatment yielded binding of $\alpha_{IIb}\beta3^{T329C/A347C}$ indistinguishable from that of the DTT-treated wild type receptor, suggesting that DTT treatment could release the disulfide bond, which locked the receptor in the low avidity state. On the other hand, the high affinity $\alpha_{IIb}\beta_3^{V332C/M335C}$ mutant adhered to immobilized fibrinogen at coating concentrations as low as 0.3 μg/ml, and DTT treatment did not alter its binding avidity, consistent with the results for soluble ligand binding.

Ligand-induced Binding Site (LIBS) Epitope Expression—Priming and ligand binding alter the conformation of $\alpha_{IIb}\beta_3$, resulting in the exposure of so-called LIBS. Such epitopes are buried in the bent conformation in interfaces between the headpiece and tailpiece and between the α leg and β leg and are exposed in the extended conformation (4, 7). To probe the conformational state of the $\alpha_{IIb}\beta_3$ mutants, binding of a panel of anti-LIBS mAbs was determined. The mAbs LIBS1 (anti-β_3; residues 420–690), LIBS6 (anti-β_3; residues 602–690), and PMI-1 (anti-α_{IIb}; residues 844–859) bound poorly to the cells stably expressing wild-type $\alpha_{IIb}\beta_3$ in Ca^{2+} but bound maximally to $\alpha_{IIb}\beta3$ activated with Mn^{2+} and RGD peptide (Fig. 5). DTT treatment for 30 min at 20 °C increased to different extents the binding of the mAbs LIBS1, LIBS6, and PMI-1 to wild type $\alpha_{IIb}\beta_3$ (Fig. 5), consistent with the ability of the DTT to partially activate the receptor. Activation with Mn^{2+} and RGD

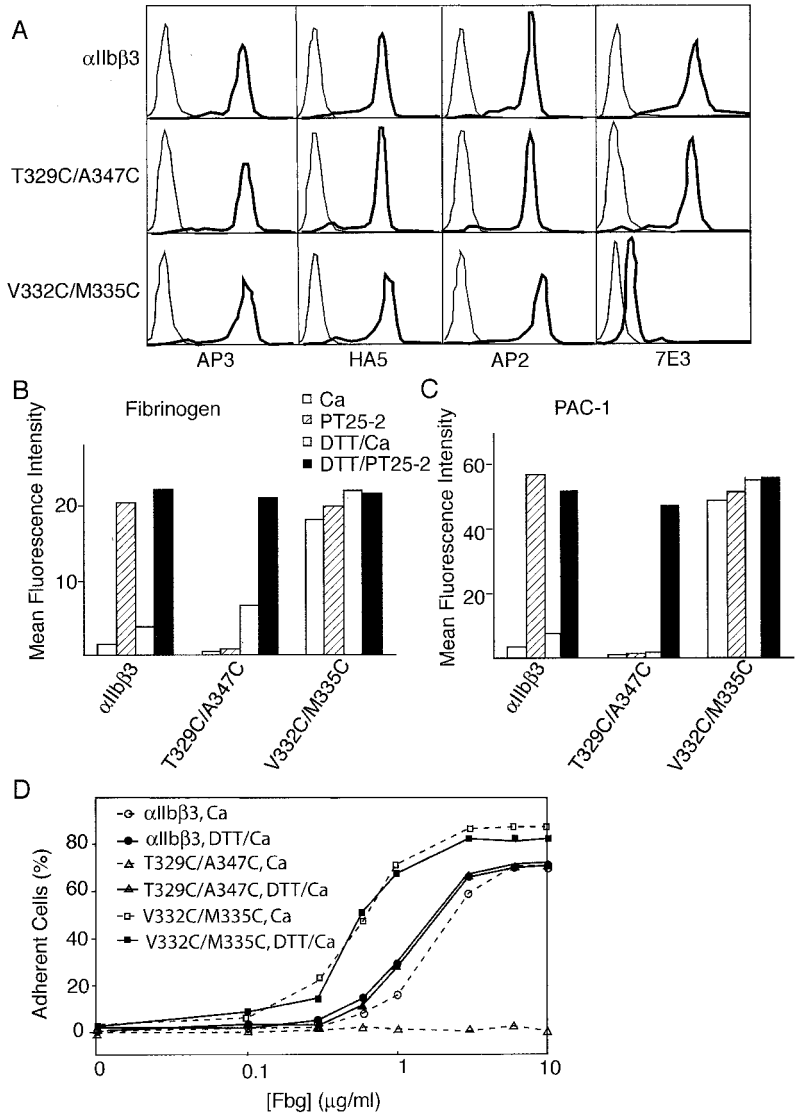

FIG. 4. **Expression and ligand binding activity of mutant $\alpha_{IIb}\beta_3$ integrins on CHO-K1 transfectants.** *A*, immunofluorescent staining. Staining of specific transfectants (*thick lines*) is compared with mock transfectants (*thin lines*). *B* and *C*, soluble fibrinogen (*B*) and PAC-1 mAb (*C*) binding. Cells were incubated with ligands in the presence of 5 mM Ca^{2+}, 1 mM Ca^{2+} plus 10 μg/ml PT25-2 mAb, 5 mM Ca^{2+} plus 5 mM DTT, or 1 mM Ca^{2+} plus 10 μg/ml PT25-2 and 5 mM DTT at room temperature for 30 min. Binding was determined as described under "Materials and Methods" as mean fluorescence intensity. *D*, adhesion of CHO transfectants in the presence of 5 mM Ca^{2+} or 5 mM DTT plus 5 mM Ca^{2+} to surfaces coated with fibrinogen at the indicated concentrations. Binding of fluorescently labeled transfectants was determined as described under "Materials and Methods." Data are representative of three independent experiments, each in quadruplicate. S.D. values were on average 1.3% and always less than 4.6%.

peptide resulted in maximal exposure of LIBS epitopes, with or without DTT treatment. By contrast, LIBS exposure in the low affinity $\alpha_{IIb}\beta_3^{T329C/A347C}$ mutant was either blunted or absent in response to RGD plus Mn^{2+} (Fig. 5). This suggests that the low affinity, disulfide-bonded, mutant receptor is in the overall bent conformation and is largely resistant to Mn^{2+}/RGD activation. DTT treatment of this mutant rescued expression of LIBS1, LIBS6, and PMI-1 epitopes in response to Mn^{2+} and RGD peptide. For the open mutant $\alpha_{IIb}\beta_3^{V332C/M335C}$, the exposure of LIBS1, LIBS6, and PMI-1 epitopes behaved similarly to wild type. The LIBS mAbs bound poorly to the mutant in Ca^{2+}, but Mn^{2+}/RGD fully exposed the epitopes. Therefore, the high affinity mutant is in an overall bent conformation. These findings suggest that the high affinity ligand binding of mutant $\alpha_{IIb}\beta_3^{V332C/M335C}$ is due to local conformational change within the I-like domain. Other LIBS mAbs including D3 (anti-β_3, residues 422–490) and AP5 (anti-β_3, residues 1–6) gave similar results (data not shown).

DISCUSSION

We have tested the hypothesis that axial displacement of the C-terminal, α7-helix of the I-like domain in integrin β subunits regulates affinity for ligand by a mechanism analogous to that previously demonstrated for I domains in integrin α subunits. As reviewed in the Introduction, there is controversy as to whether the position of the α7-helix visualized in crystal structures corresponds to a low or high affinity conformation and whether the position of the α7-helix moves during conformational regulation of affinity. We present two independent tests of the hypothesis that the conformation of the α7-helix seen in crystal structures stabilizes integrins in a low affinity conformation and that the helix is displaced during activation: 1) a disulfide designed to lock the α7-helix in the same position as in crystal structures should stabilize the low affinity state; 2) a disulfide designed to displace the β6-α7 loop in the C-terminal, axial direction should activate the high affinity state. Both experimental tests support the hypothesis, with the first test providing particularly strong support because the functional effects of disulfide formation were reversible upon reduction, and a crystal structure rather than a hypothetical model was available for designing where the cysteines were introduced.

The formation of each of the introduced disulfide bonds, Cys^{329}–Cys^{347} to stabilize the low affinity conformation and Cys^{332}–Cys^{335} to stabilize the high affinity conformation, was directly demonstrated by a shift in mobility in nonreducing SDS-PAGE and by quantitating free sulfhydryls with biotinylation. An interesting sidelight is that we find a background level of ~0.3 free sulfhydryls per β_3 subunit in the mature $\alpha_{IIb}\beta_3$ complex labeled under native conditions. This might appear to contradict a recent report that resting and activated conformers of $\alpha_{IIb}\beta_3$ isolated from outdated human platelets

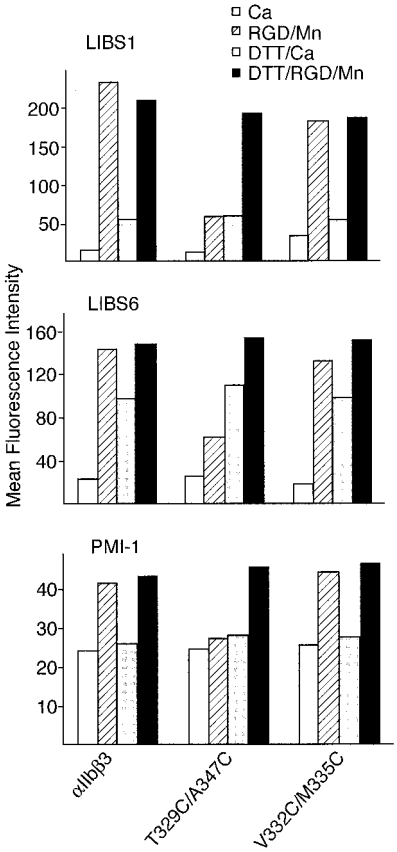

FIG. 5. **Exposure of LIBS epitopes.** Wild-type and mutant CHO transfectants were incubated in the presence of 5 mM Ca^{2+}, 1 mM Mn^{2+} plus 100 μM GRGDSP (RGD) peptide, 5 mM DTT plus 5 mM Ca^{2+}, or 5 mM DTT plus 1 mM Mn^{2+} and 100 μM GRGDSP (RGD) peptide for 30 min at room temperature and then with mAbs on ice for 30 min. Binding was determined with FITC anti-IgG as described under "Materials and Methods."

contain 2.6 and 4.4 free cysteines per β_3 subunit labeled under denaturing conditions, respectively, and that disulfide exchange is involved in integrin activation (25). However, early studies on $\alpha_{IIb}\beta_3$ either isolated from platelets and labeled under denaturing conditions or labeled with sulfhydryl reagents under native conditions on intact platelets found no free sulfhydryls in the α_{IIb} or β_3 subunits, whereas the one free sulfhydryl in the cytoplasmic domain of platelet GpIb was detected (26, 27). Therefore, our results are in good agreement with the earlier studies.

The disulfide formed in the $\beta_3^{T329C/A347C}$ mutant stabilized the low affinity state of $\alpha_{IIb}\beta_3$. Thr^{329} and Ala^{347} are located within the beginning portion of the β6-strand and within the last portion of the α7-helix, respectively, much closer to the "bottom" of the I-like domain that connects to the hybrid domain than to the "top" of the I-like domain that binds ligand. There is no significant difference in the positions of these residues between the unliganded and liganded $\alpha_V\beta_3$ crystal structures (5, 6), and their positions are such that when substituted with cysteine, disulfide bond formation should result in little or no local structural rearrangement. The Cys^{329}–Cys^{347} disulfide bond locked $\alpha_{IIb}\beta_3$ in the low affinity conformation, as shown by lack of binding to soluble fibrinogen or PAC-1 mAb, with or without activation. It was interesting that $\alpha_{IIb}\beta_3^{T329C/A347C}$ was also incapable of mediating adhesion of transfectants to fibrinogen on substrates, which does not require activation. In this assay, binding to ligand may occur as a consequence of the high local concentration of ligand, and ligand binding may drive the shift in the equilibrium from the low to the high affinity conformation of the receptor.

The $\alpha_{IIb}\beta_3^{T329C/A347C}$ mutant remained in the bent conformation as shown by lack of activation epitope exposure. It was also largely resistant to activation epitope exposure by RGD peptide and Mn^{2+}. The functional effects of disulfide bond formation were completely reversible by DTT reduction, with DTT-treated $\alpha_{IIb}\beta_3^{T329C/A347C}$ behaving identically to DTT-treated wild type $\alpha_{IIb}\beta_3$. We conclude that in crystal structures determined to date, the β_3 I-like domain is in the low affinity state, and for conversion to the high affinity state, a substantial movement in the position of the side chain of Ala^{347} relative to that of Thr^{329} is required. The position of Thr^{329} is largely fixed by its location within a β-strand with numerous backbone hydrogen bonds to the central I-like domain β-sheet, and therefore the data are most consistent with a movement of the α7-helix containing Ala^{347}.

Results with the $\alpha_{IIb}\beta_3^{V332C/M335C}$ mutant specifically support a conformational change in the β6-α7 loop as an activation mechanism. The β6-α7 loops of integrin β I-like and α I domains have a different number of residues, and it is therefore difficult to model rearrangement of the I-like β6-α7 loop. It is also not clear whether downward movement of the α7-helix in β I-like domains would involve one or two turn displacements as found in the intermediate and open conformations of I domains, respectively (16). Therefore, it is difficult to know whether the change in the β6-α7 loop induced by disulfide formation between Cys^{332} and Cys^{335} will accurately mimic physiologic rearrangement of this loop. Nonetheless, the position of residue 332 is largely fixed by its position in the β6-strand and the backbone hydrogen bonds between the β5 and β6 strands. Therefore, the backbone rearrangement required to form the Cys^{332}-Cys^{335} disulfide bond is almost certain to come from a downward displacement of the β6-α7 loop, bringing Cys^{335} into position to form the disulfide bond with Cys^{332} that was directly demonstrated here by chemical labeling studies. The $\alpha_{IIb}\beta_3^{V332/M335C}$ mutant was constitutively active in soluble ligand binding assays and appeared to be maximally activated. The mutant was also highly active in adhesion to fibrinogen. The activity of the $\alpha_{IIb}\beta_3^{V332C/M335C}$ mutant was not reversed by reduction. It is likely that the Cys^{332}-Cys^{335} disulfide bond is resistant to reduction, like most wild type β_3 disulfides; however, we cannot rule out the possibility that both the disulfide bond and the combination of two free cysteines at positions 332 and 335 are activating, although each single cysteine is not. A converse result was obtained in a similar study on α_L I domains; a disulfide designed to stabilize the high affinity conformation was reversible by DTT, whereas a disulfide designed to stabilize the low affinity conformation was not reversible with DTT (13, 14, 17).

The high affinity $\alpha_{IIb}\beta_3^{V332C/M335C}$ mutant did not constitutively express activation epitopes, but these were induced upon treatment with RGD peptide and Mn^{2+}. An analogous result was obtained with an α_L I domain locked in the high affinity state with a disulfide bond (14). Subsequent crystal structure studies on the isolated, high affinity α_L I domain demonstrated that the C-terminal α7-helix had indeed been displaced downward by the disulfide bond introduced into the β6-α7 loop, although there was some deformation of the α7-helix by the mutation (16). The intact, high affinity $\alpha_L\beta_2$ heterodimer remained in the bent conformation, and extension was activated by Mn^{2+}, as revealed by mAb to LIBS or activation epitopes. The interpretation for the α_L I domains is that the α7-helix should not be viewed as a rigid rod but rather as a spring or a rope; in other words, some looping out may occur so that a downward movement of the α7-helix in the I domain is not necessarily transmitted to other integrin domains (14). Simi-

larly, after introduction here of the Cys^{332}–Cys^{335} disulfide between the β6-strand and the β6-α7 loop, the local conformational change in this loop did not appear to be transmitted to a change in orientation between the I-like and hybrid domains, as revealed by lack of LIBS epitope exposure. This suggests that the α7-helix in the β I-like domain may also behave as a spring or rope, with conformational change in the β6-α7 loop not necessarily communicated to downward movement at the bottom of the α7-helix, perhaps because of bulging out of the α7-helix or the connection between the β6-α7 loop and the α7-helix. Movements of the adjacent β I-like α1- and α2-helices have also been implicated in integrin activation (5, 10), and concerted movements of the α1-, α2-, and α7-helices may be required for full linkage of the affinity state of the β I-like MIDAS to the I-like domain interface with the hybrid domain and explain the ability of RGD peptide plus Mn^{2+} to activate LIBS epitope exposure in the $\alpha_{IIb}\beta_3^{V332C/M335C}$ mutant.

Taken together, the results with the $\alpha_{IIb}\beta_3^{T329C/A347C}$ and $\alpha_{IIb}\beta_3^{V332C/M335C}$ mutations strongly support the importance of β I-like domain α7-helix movement in integrin affinity regulation. Both hypothesis-driven mutations in the β I-like domain had the predicted effect. One, designed to displace the β6-α7 loop downward, indeed activated ligand binding. The other, designed to hold the β6-strand and α7-helix together near the end of the α7-helix, indeed maintained $\alpha_{IIb}\beta_3$ in the low affinity state and demonstrated that this relative arrangement of these two secondary structure elements, visualized in crystal structures (5, 6), corresponds to the low affinity state. Together, the results with the two mutations support the hypothesis that C-terminal α7-helix displacement increases affinity for ligand but do not rule out the possibility that additional movements are also involved in linking the high affinity state of the ligand binding site to movements at the I-like domain interface with the hybrid domain and LIBS epitope exposure.

Integrins are important therapeutic targets in many inflammatory and vascular disorders. The rational design of mutations that allosterically stabilize high affinity or low affinity conformations of integrins demonstrates marked advances in our understanding of the molecular basis of affinity regulation. This progress also holds out the promise that drugs might be designed that stabilize the low affinity conformation of integrins, in contrast to the current generation of "ligand-mimetic" integrin antagonists that stabilize the high affinity conformation.

Acknowledgments—We thank Drs. M. H. Ginsberg and S. Shattil for generously providing antibodies. We thank Aideen Mulligan for laboratory management assistance and Jessica Martin for secretarial assistance.

Note Added in Proof—Deletion of one turn (4 residues) of the α7-helix of the β_2 and β_7 I-like domains also activates ligand binding, independent of the position of this deletion in the α7-helix. This result further supports the hypothesis that downward movement of the α7-helix activates integrins (Yang, W., Shimaoka, M., Chen, J. F., and Springer, T. A. (2004) *Proc. Natl. Acad. Sci. U. S. A.*, in press).

REFERENCES

1. Hynes, R. O. (2002) *Cell* **110,** 673–687
2. Shimaoka, M., Takagi, J., and Springer, T. A. (2002) *Annu. Rev. Biophys. Biomol. Struct.* **31,** 485–516
3. Kim, M., Carman, C. V., and Springer, T. A. (2003) *Science* **301,** 1720–1725
4. Takagi, J., Petre, B. M., Walz, T., and Springer, T. A. (2002) *Cell* **110,** 599–611
5. Xiong, J. P., Stehle, T., Zhang, R., Joachimiak, A., Frech, M., Goodman, S. L., and Arnaout, M. A. (2002) *Science* **296,** 151–155
6. Xiong, J.-P., Stehle, T., Diefenbach, B., Zhang, R., Dunker, R., Scott, D. L., Joachimiak, A., Goodman, S. L., and Arnaout, M. A. (2001) *Science* **294,** 339–345
7. Beglova, N., Blacklow, S. C., Takagi, J., and Springer, T. A. (2002) *Nat. Struct. Biol.* **9,** 282–287
8. Takagi, J., Strokovich, K., Springer, T. A., and Walz, T. (2003) *EMBO J.* **22,** 4607–4615
9. Luo, B.-H., Springer, T. A., and Takagi, J. (2003) *Proc. Natl. Acad. Sci. U. S. A.* **100,** 2403–2408
10. Mould, A. P., Askari, J. A., Barton, S., Kline, A. D., McEwan, P. A., Craig, S. E., and Humphries, M. J. (2002) *J. Biol. Chem.* **277,** 19800–19805
11. Mould, A. P., Barton, S. J., Askari, J. A., McEwan, P. A., Buckley, P. A., Craig, S. E., and Humphries, M. J. (2003) *J. Biol. Chem.* **278,** 17028–17035
12. Mould, A. P., Barton, S. J., Askari, J. A., Craig, S. E., and Humphries, M. J. (2003) *J. Biol. Chem.* **278,** 51622–51629
13. Lu, C., Shimaoka, M., Ferzly, M., Oxvig, C., Takagi, J., and Springer, T. A. (2001) *Proc. Natl. Acad. Sci. U. S. A.* **98,** 2387–2392
14. Lu, C., Shimaoka, M., Zang, Q., Takagi, J., and Springer, T. A. (2001) *Proc. Natl. Acad. Sci. U. S. A.* **98,** 2393–2398
15. Shimaoka, M., Lu, C., Palframan, R., von Andrian, U. H., Takagi, J., and Springer, T. A. (2001) *Proc. Natl. Acad. Sci. U. S. A.* **98,** 6009–6014
16. Shimaoka, M., Xiao, T., Liu, J.-H., Yang, Y., Dong, Y., Jun, C.-D., McCormack, A., Zhang, R., Joachimiak, A., Takagi, J., Wang, J., and Springer, T. A. (2003) *Cell* **112,** 99–111
17. Shimaoka, M., Lu, C., Salas, A., Xiao, T., Takagi, J., and Springer, T. A. (2002) *Proc. Natl. Acad. Sci. U. S. A.* **99,** 16737–16741
18. Lee, J.-O., Rieu, P., Arnaout, M. A., and Liddington, R. (1995) *Cell* **80,** 631–638
19. Emsley, J., Knight, C. G., Farndale, R. W., Barnes, M. J., and Liddington, R. C. (2000) *Cell* **101,** 47–56
20. Levitt, M. (1992) *J. Mol. Biol.* **226,** 507–533
21. DuBridge, R. B., Tang, P., Hsia, H. C., Leong, P. M., Miller, J. H., and Calos, M. P. (1987) *Mol. Cell Biol.* **7,** 379–387
22. Huang, C., and Springer, T. A. (1997) *Proc. Natl. Acad. Sci. U. S. A.* **94,** 3162–3167
23. Lu, C., and Springer, T. A. (1997) *J. Immunol.* **159,** 268–278
24. Puzon-McLaughlin, W., Kamata, T., and Takada, Y. (2000) *J. Biol. Chem.* **275,** 7795–7802
25. Yan, B., and Smith, J. W. (2000) *J. Biol. Chem.* **275,** 39964–39972
26. Eirin, M. T., Calvete, J. J., and Gonzalez-Rodriguez, J. (1986) *Biochem. J.* **240,** 147–153
27. Kalomiris, E. L., and Coller, B. S. (1985) *Biochemistry* **24,** 5430–5436
28. Guex, N., and Peitsch, M. C. (1997) *Electrophoresis* **18,** 2714–2723
29. Carson, M. (1997) *Methods Enzymol.* **277,** 493–505